Flexible digital manufacturing of timber construction: the design and fabrication of a free-form nexorade

Romain Mesnil, Tristan Gobin, Leo Demont, Pierre Margerit, Nicolas Ducoulombier, Cyril Douthe, Jean-François Caron

Flexible digital manufacturing of timber construction: the design and fabrication of a free-form nexorade

Romain Mesnil[1*], Tristan Gobin[1,2,3], Leo Demont[1], Pierre Margerit[1], Nicolas Ducoulombier[1], Cyril Douthe[1] and Jean-François Caron[1]

[1*]Laboratoire Navier, Ecole des Ponts, Université Gustave Eiffel, CNRS, Champs-sur-Marne, France.
[2]Laboratoire GSA, Ecole Nationale Supérieure d'Architecture Paris Malaquais, Paris, France.
[3]HAL Robotics Ltd, London, United Kingdom.

*Corresponding author(s). E-mail(s): romain.mesnil@enpc.fr;

Abstract

This article investigates the application of a multi-robotic platform to the fabrication of complex "free-form" timber structures. A concept of *"smart factory"*, with a 13-DOF robotic cell combining robotic mobility with fixed workstations, is proposed. A computational workflow was implemented to allow for fast iterations during the early design stage. The robotic cell design and design workflow are implemented in practical experiments conducted in the framework of intensive workshops. A productivity assessment is performed on a 50 m^2 pavilion prefabricated with the proposed robotic cell.

Keywords: robot-oriented design robotic timber construction non-standard structures nexorade reciprocal frame reciprocal structure form-finding planar meshes

1 Introduction

1.1 Context

Robotics challenges today's architects and engineers, as it opens new possibilities for the fabrication and assembly of custom-made building components [1]. Based on the trend of the last two centuries, one can expect innovative structural systems to emerge after the recent breakthrough in large-scale robotic construction [2, 3, 4]. New processes, like additive manufacturing, already disrupt the automotive and aeronautic industries, by blurring the differences between material, micro-structure and object [5]. Similar innovations can be expected with robotized subtractive manufacturing.

Concurrently, there is a movement towards design rationalization for complex envelopes and structures through discrete geometry [6, 7, 8, 9]. The rationalization of non-standard architecture is well-established in practice and is still an active research topic in academia. Practical restrictions results from the machining tool capabilities, which are more difficult to express as geometrical constraints [10]. These limitations are rarely included in the early stages of design or in scholarly studies dealing with *fabrication-aware design*, resulting in a gap between design workflow and production.

This paper aims to question the opportunity of using robotic fabrication for complex (or non-standard) timber structures and envelopes. The notion of *Robot-Oriented Design* (ROD), which proposes a concurrent design of the building components and the manufacturing tools, is used to tackle the limitations of current fabrication-aware design approaches. The relationship between rationalization techniques and machining tools in the design workflow is assessed through a detailed case study of the design and construction of complex timber structures.

1.2 Previous work

1.2.1 Robot-Oriented Design

Thomas Bock introduced the concept of Robot-Oriented Design (ROD) in 1988 in his doctoral thesis [11]. A recent series of books [12, 13, 14] describes this methodology and gathers operational research and perspectives on robotics in civil engineering. ROD is a design methodology that aims to integrate robotic constraints into the design of building components. One of its main objectives is to decrease on-site construction time by applying lean manufacturing and robotics. The whole life-cycle of the building is considered in ROD, which can be seen as a synthesis of *"Design for X"*, from manufacturing (Design for Manufacturing) to construction (Design for Assembly [15]), to the end-of-life (Design for Reuse [16]). The environmental footprint of buildings and their pressure on material consumption and the global carbon footprint make this design approach even more compelling in the twenty-first century.

1.2.2 Design of structures with complex geometries

The embedding of fabrication constraints in the design process of doubly-curved building structures and envelopes is an important aspect of a research field called *architectural geometry* [6]. However, architectural geometry rarely considers machinery limitations, because they are by definition diverse (each machine or process comes with specific limitations) and thus more difficult to generalize. For example, the size of a robot is a practical constraint that imposes a limitation on the dimensions of manufactured items. Constraints on the dimensions of building components are difficult to handle, as illustrated in recent research on constant-length beam networks on curved surfaces [17, 18]. Conversely, with ROD being mainly focused on industrialization and mass production, few works on architectural geometry have been integrated into this workflow. Therefore, finding a compromise between a ROD approach and advanced geometrical principles for construction rationalization is still a vastly open research route, as pointed out by Austern *et al.* [10].

1.2.3 Architectural applications of robotics for complex structures

The timber industry mainly uses CNC to perform complex milling operations [15]. Those highly specialized machines are extremely precise and are arguably more productive and robust than industrial manipulators for specialized tasks, but they are not affordable for small companies and are not as versatile as industrial robots, which can be used in a multi-process context.

The majority of current research on construction robots attempts to overcome this difficulty by aiming for greater flexibility or by using industrial manipulators for particular jobs that are still not automated in industrial CNC. More and more initiatives integrating robotics, sensors, and architectural engineering within complex timber projects emerge with research pavilions [19].

The technological modalities differ, from 3D scanning combined with robotic milling [20], wood bending with synchronous robots [21], to the assembly of complex wood lattice [22] or reciprocal frames [23] by robotic manipulators. The emergence of parametric design and robot frameworks tailored for the construction industry [24, 25] allowed such explorations. More recently, Wagner *et al.* designed a modular cell using two robots and a turntable [26] to build the complex timber cassettes of the BUGA Pavilion.

1.2.4 Prefabrication automation for timber structures

Timber construction relies on prefabrication with CNC systems. This makes timber one of the most mature construction materials for automation. Timber structures are characterized by a wide variety of assembly strategies that come with

specific manufacturing constraints. Figure 1 shows the three main strategies for connection.

- glued connections, which are difficult to implement on-site;
- friction-based connections, which can range from simple half-lapped joints to more complex interlocked patterns [27];
- mechanical connections, using nails or screws, which can be combined with tenons and mortises [28].

Some projects with glued connections only require simple cuts of timber beams [29], while friction-based assembly may require complex machining operations. Recent advances in digital manufacturing have resulted in the rediscovery of ancient construction techniques like integral wooden attachments [30, 31], or nexorades [32, 33].

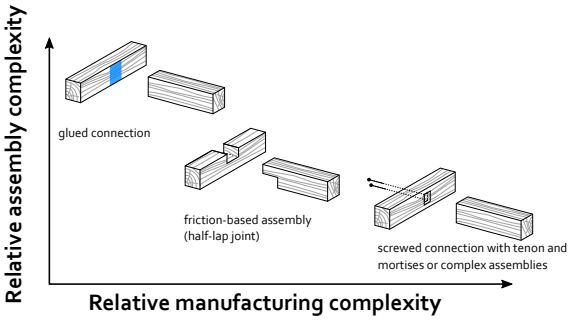

Fig. 1 Conceptual classification of some assembly strategies for timber structures

Non-standard projects with complex timber structures have been completed thanks to workflow digitization and automation from design to fabrication [34]. Novel concepts for assemblies taking advantage of new robot architectures have been successfully applied to timber structure assembly [35].

1.3 Problem statement

The literature review highlights multiple contributions towards the automation of timber construction, either through manufacturing or assembly. Although the need for the versatility of the robotic cell has been acknowledged [36], most of the literature focuses on a single process. By designing an adaptable robotic cell, this paper hopes to contribute to the design of flexible factories for timber buildings. This robotic cell was used to create a wooden pavilion.

Section 1 introduced the literature on the topic of robotic timber construction. Section 2 presents a methodology to handle complexity in free-form timber structures with a modular robotic cell. Section 3 presents a case study of a 50m^2 pavilion. Section 4 presents a productivity assessment of this case study. The paper concludes with a discussion of the scalability and generality of the method.

2 Methodology: Design of a modular factory

2.1 Motivation

The flexibility of the industrial automation system, either through modularity or interchangeability, is a key aspect of construction automation [12]. Traditional (non-automated) off-site construction initially focused on component modularity and simplification, going hand-in-hand with the ideas of American modernism, which progressively led to the disappearance of architectural ornaments [37]. Construction automation is now seen as a means of reintroducing complexity in the modules themselves. Bock and Linner list numerous examples of automated module fabrication in their monographs, from bathroom complexes to building units, where complexity is used to solve problems (like assembly or maintenance) [38]. Construction robotics can be used to construct free-form projects, with high component customization. Conversely, some highly specialized machinery can be used, but at the cost of over-specialization and low adaptability. Reconfigurability has, however, been identified as a key aspect of so-called *smart factories* [39]. Indeed, Hozdić defines smart factories as *"a manufacturing solution that provides such flexible and adaptive production processes that will solve problems arising on a production facility with dynamic and rapidly changing boundary conditions in a world of increasing complexity"* [40]. Therefore, the notion of modularity shifts towards *factory modularity*. This requires several innovations: software (high interoperability between BIM and robotics cells), hardware (for example, through robot mobility and hardware modularity), and organisational

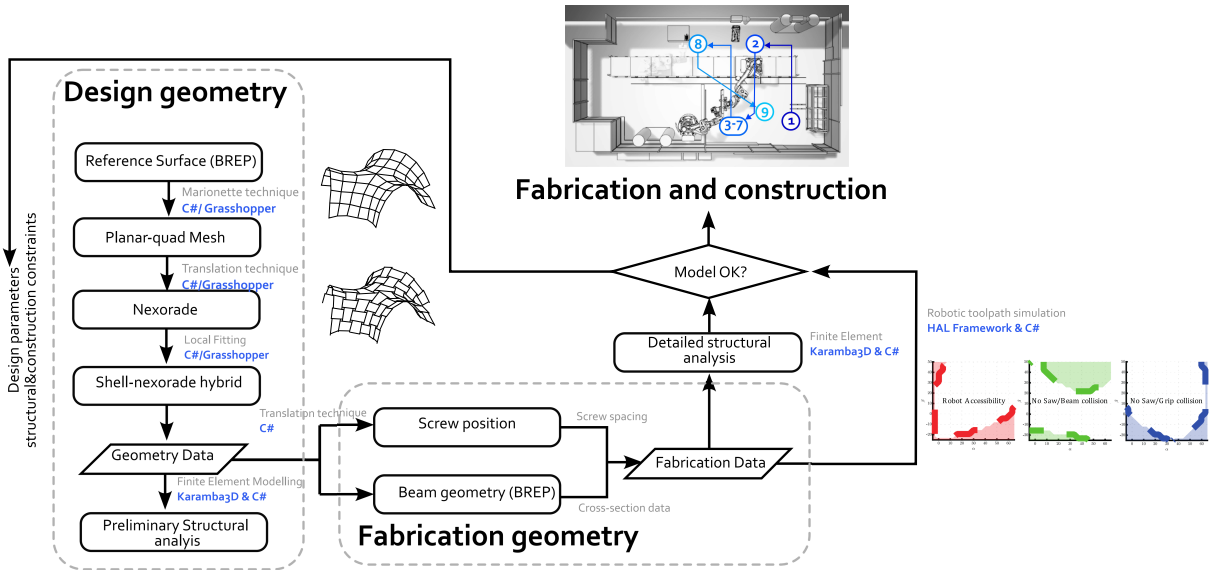

Fig. 2 Digital workflow of the timber pavilion presented in Section 3.

innovations in the project. These three aspects are treated in this article.

2.2 Modularity through software integration

The production of an architectural artifact depends not only on the means of production, but also on how we control them, and how to connect information embedded in the design. The integration of a workflow between Computer-Aided Design (CAD) and Computer-Aided Manufacturing (CAM) has already been discussed in [41]. Proprietary software solutions allow the creation of a digital twin of the robotic cell and the simulation of complex operations, like milling. However, the feedback loop between manufacturing and design might be difficult in practice, due to the time required to generate CAM file, which is incompatible with true interaction between humans and computers. Indeed, Shneiderman identified that repetitive design tasks should be made in less than one second to keep the human engaged in the design process and benefit from the feedback of the machine [42].

To avoid this problem, our recommended design approach relies on object-oriented programming. Each part or component of the architectural artifact is described as an object, with increasing informational complexity as one comes closer to fabrication. This enables faster iterations in the early stages of design, where many constraints are handled at once [43]. The graph-based modeling approach used by Isaac *et al.* [44] is another example of a modeling approach allowing this notion of informational granularity in prefabrication automation.

The manipulation of objects also implies the labeling of details and operations (milling, drilling, etc.). Although it is possible to define a specific CAD/CAM interface for a construction project, interoperability with existing CAM formats, like BTL, should be considered. Promising steps in this direction have been made in [45], with the creation of a Grasshopper plug-in exporting CAD information into BTL. Other software solutions integrate robot and sensor catalogs, allowing the configuration of a cell without being tied down to a particular robotic brand [24].

Figure 2 presents a brief overview of a possible digital workflow, implemented in the third section of this article. The first stage of the design is the

form-finding *design geometry*, where the designer starts by generating a free-form in a traditional CAD environment, in our case, Rhinoceros and Grasshopper. Some constraints, like panel planarity, can be embedded early in form-finding. The designer may perform a form-fitting under a planarity constraint, or embed the fabrication constraint into the form-finding tool, without the need for reference geometry. A simplified finite element analysis can be performed to check the feasibility of the design during the first design iterations. At this stage, the model contains little information and design iterations can be extremely fast: a planarization can merely take milliseconds [46], while a finite element analysis with beam elements takes less than a second. The second stage, labeled *Fabrication geometry* in Figure 2 consists in creating a detailed geometry that can be used as an input for a robotic tool-path simulation software. Specific geometrical data (like the position of neutral axes of beams and cross-sections) can also be used in a detailed structural analysis. Finally, the feasibility according to the more detailed structural analysis and robotic fabrication is assessed. Design iterations during this stage are significantly more time-consuming, because of the growing level of detail in the representation of the objects. In the case study presented in the next section, the simulation of all fabrication steps for one beam took between 1 and 2 minutes, and the simulation of the fabrication of the whole pavilion was computed in 3 hours.

For projects with few components, this design loop may be completely integrated into a single parametric software package. However, it is possible to use the *fabrication geometry* stage to construct simplified feasibility metrics that can be used in the *design geometry* stage. An example of such an approach is explained in Section 3.3.2. Automated generation of robotic tool-path allows to optimize the flexibility and performance of the robotic cell, but also to understand its practical limitations and inform the designer on the feasibility of a design. Therefore, the design workflow is compatible with the ROD approach, which considers robotic constraints in the design process.

2.3 Flexibility through mobility

Mobility is an essential aspect of the reconfigurability of factories. The spread of automated guided vehicles (AGV) across almost all industries is illustrative of this trend [47]. Mobility can be achieved through the mobility of the parts, for example, with a conveyor belt [48], a turning table [35] or an AGV, or by robot mobility, on a track or an AGV. Finally, recent industrial and academic projects have focused on robotic cell mobility to bring fabrication units closer to the building site [49, 36].

This article uses a compromise between these two options with a pneumatic gripper on a mobile robot (on a track) that navigates through the cell, shown in Figure 3, to reach various workstations, one of those being a fixed 6-axis robot. The mobile robot thus acts as a reference frame for the gripped part.

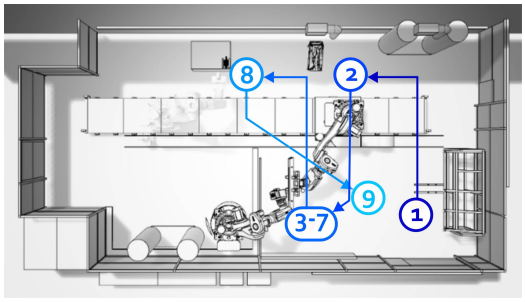

Fig. 3 Top view of the robotic cell and the various workstation: feeder (1), rough cut (2), milling (3-7), drilling (8), deposition (9).

2.4 Modularity through end-effector

Lastly, modularity of the micro-factory is achieved with modular tooling: automated pneumatic tool changers by Schunk allow for fast tool change and cell reconfiguration [50]. Only a few minutes are required to change a tool with this setup. It is thus possible to reconfigure the cell to perform milling, complex assembly, or quality control.

3 Robot-oriented design of a complex nexorade structure

This section presents the design and fabrication strategy of a free-form timber structure, built in 2017.

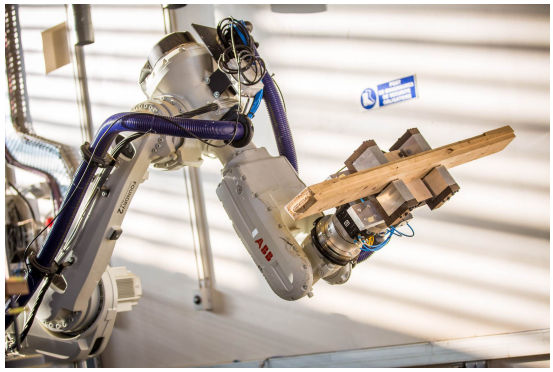

Fig. 4 Modular end effector: automatic tool changer and gripper with adjustable bits (credit: Ecole des Ponts ParisTech/Stefano Borghi).

3.1 Design intent and constraints

The case study concerns a nexorade [32], also known as a reciprocal structure. This structural system uses short members, which are assembled in *fans*. By design, the only connections between beams are bivalent, which is significantly simpler to assemble and manufacture than complex nodes in free-form gridshells [4]. Nexorades are thus an interesting structural system in the context of prefabrication and automation, which focuses on simplicity and standardization of assembly [44].

The family of nexorades can be extended to *shell-nexorade hybrids*, which are nexorades braced by planar panels. The main benefit of shell-nexorade hybrids is their excellent structural performance, comparable to shell structures, while traditional nexorades remain *bending dominated structures*, with a span restricted to a few meters. The case study presented in this paper is the digital fabrication of the first shell-nexorade hybrid structure, shown in Figure 5. Each beam-to-beam interface has a valency of two, and each beam is attached to two panels.

The pavilion consists of 102 beams and 48 panels, which are all unique. Like many free-form structures, there is thus a large variety of components that requires versatility in the means of production.

3.2 Component geometry

The pavilion was constructed in the framework of an intensive workshop [51], with low-skilled labor for assembly. The case study investigates a screwed connection with tenons and mortises, shifting the complexity from the assembly to the manufacturing process. The construction scenario is an assembly of small individual components, shown in Figure 6. There are three types of interfaces for a typical beam:

- at both ends, a connection to other beams, highlighted in red;
- on the same side, a connection to other beams, marked in orange;
- at the top, connections to two panels, identified in blue.

A ruled surface, shown in green, is milled to provide a smooth visual transition between panels and beams on top of the surface ("roof" of the pavilion). While not functionally necessary, it greatly improves structural aesthetics.

The beam-to-beam connections are made with screws, pilot holes are drilled robotically, while tenons and mortises are used as guides during assembly, and are not perfectly adjusted, with a 0.5mm clearance. Beam-to-panel connections are realized with grooves, which act as a fail-safe during assembly, providing alignment between the top of a panel and the beam. The grooves are sections of planes, but they have an arbitrary orientation, as shown in Figure 7. They have a depth of 10.5 mm and a width of 20 mm, which allows the use of screws for the mechanical connection between panels and beams. Beams have a length comprised between 1,200 mm and 1,800 mm.

Figure 6 illustrates the high geometrical complexity of components and the large number of features (tenons, mortises, holes, rough cut) on a single member. In addition, Figure 8 highlights the fact that the bottom surface of the beams is milled to hide offsets between members resulting from the nexorade configuration. There are thus milling operations on five sides out of six on the beam. By contrast, the panels are extremely simple and can be milled with a 2D CNC machine. The complex geometry of the pavilion, shown in Figure 5, makes every beam unique, which adds difficulty to the manufacturing and quality control procedures.

3.3 Organization of the cell

The cell is composed of two robots (model: ABB IRB 66200, span: 2.2 m, payload: 150 kg). One of

Fig. 5 The shell-nexorade hybrid structure constructed (credit: Tristan Gobin).

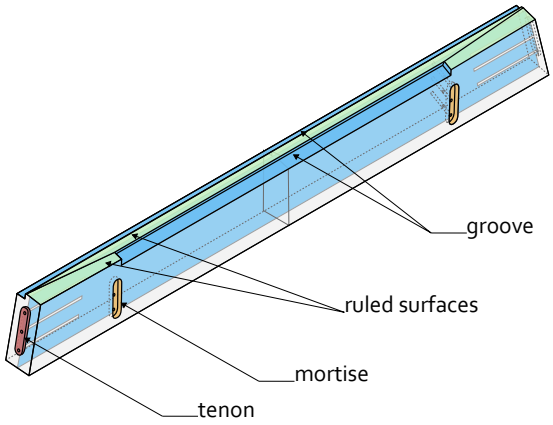

Fig. 6 Axonometric view of a beam. The three types of interfaces with other components are highlighted in blue, red, and orange.

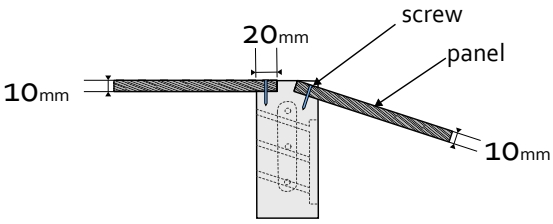

Fig. 7 Section of a beam: connection with both panels.

Fig. 8 Bottom of the pavilion. The bottom surface of beams is milled to mask offset and avoid exposure of the timber fibres (credit: Tristan Gobin).

the robots is on an 8-meter track. The cell is organized around the track, with fixed workstations corresponding to the different actions to perform:

1. Beam picking in the feeder
2. Rough cut
3. Tenons milling
4. Mortises milling
5. Ruled-surface milling
6. Grooves milling
7. Bottom surface milling
8. Pre-drilling of holes.

The robot was calibrated in a few particular places on the track that corresponded to the machining positions. One of the constraints was to select as few positions of the robot on the track as possible for steps 2–7, to guarantee precision.

3.3.1 Beam picking

The feeding is illustrated in Figure 9: the feeder is oriented upwards, which guarantees the positioning of the part in the local reference plane xy. However, the positioning of the part along x may be imprecise. This is mitigated by a sawing operation, where the saw is calibrated with respect to the tool reference frame: after cutting, the ends of the beam are known (up to calibration accuracy), and the robot can perform the other tasks (3–8).

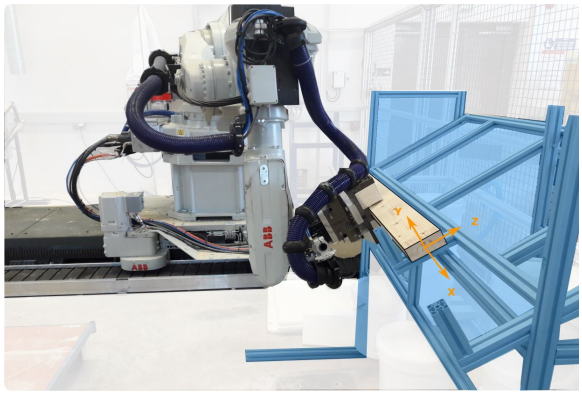

Fig. 9 Picking of a part in a feeder (blue) and local axes of the part (in orange).

3.3.2 Rough cut of a beam.

The rough cut is made with a fixed circular saw, highlighted in blue in Figure 10. Three types of critical errors have been identified when generating the tool path:

- Robot accessibility: the position cannot be reached by the robot, usually because of the eccentricity of the beam;
- collision between the beam and saw: which is due to the length of the beam (up to 2 meters before cutting);
- collision between the gripper and saw: the gripper being much wider than the beam (see Figure 4), it may collide with the saw.

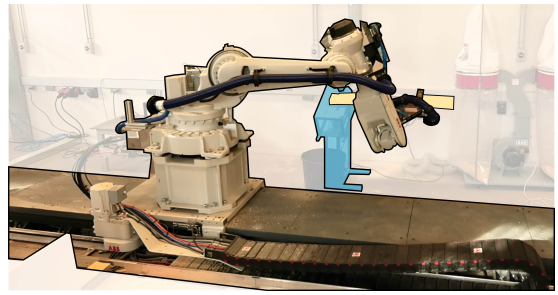

Fig. 10 Rough-cut. The circular saw support is highlighted in blue for clarity.

Figure 11 shows the three main parameters describing the rough cut: two angles α and β and a distance between the cutting plane and the centre of the gripper. Free-form structures are characterized by a variety of dimensions and orientations, and the feasibility of all beams must be verified before fabrication.

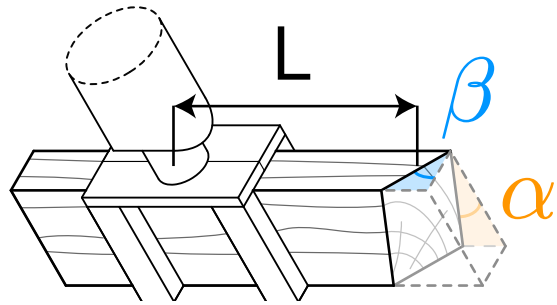

Fig. 11 Notation of the rough cut parameters for a beam.

Figure 12 shows the space of feasible solutions for $L = 0.75m$. The trajectories have been generated with HAL Robotics software by sampling integer values of (α, β). The *robot accessibility* and *saw/gripper collision* feasible domains can be approximated with good precision by convex domains, but the *saw/beam collision* domain is non-convex.

The integration of fabrication constraints thus leads to non-convex problems, which are notoriously difficult to solve in real-time. Rather than trying to simulate all trajectories for each design iteration, this map is produced before production to provide a simple feasibility criterion for the designer, who may integrate them with no computational overhead in the design workflow. It can be noticed that the value $\beta = 0$ (when the beam neutral axis is perpendicular to the saw plane) seems

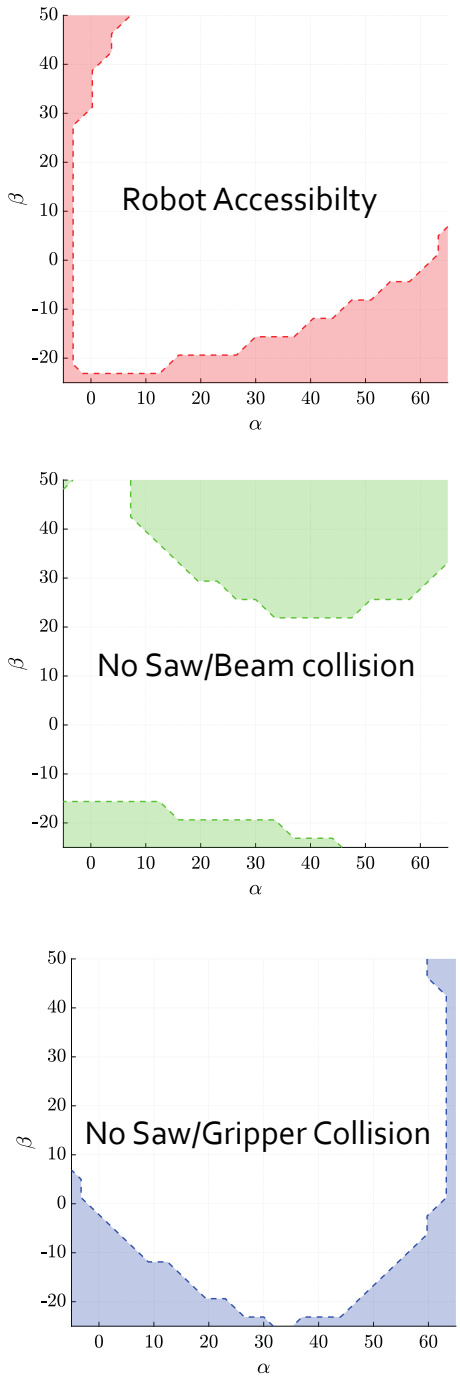

Fig. 12 Discrete sampling of the feasibility domain for parameters with $L = 0.75m$. Feasible regions are in white, while coloured regions are not feasible. Notice that the intersection of these feasible domains is non-convex.

to result in the most accessible region. This means that the beams should be as perpendicular as possible. If one combines this constraint with panel planarity, it can be concluded that the network of beams should be as close as possible to the lines of curvature of the reference surface. Fortunately, these curve networks have been thoroughly studied in the architectural geometry community, and therefore, the simulation of robotic constraint can inform the designer on the shape rationalization strategy from existing literature and numerical toolboxes [6, 7, 52, 53, 54].

3.3.3 Milling operations

The milling operations involve a collaboration between the picking robot and another 6-axis robot arm equipped with a spindle, shown in Figure 14.

Accessibility is challenging, due to potential collisions between the spindle and the gripper. Since five sides of the beam are milled, the beams are re-orientated several times through stages (3-7), as seen in Figure 13. The milling speed is also adjusted to avoid resonance dynamic loads that would lower the milling accuracy. In particular, it was observed that over-extension of the gripping robot led to resonance. The common milling area for both robots is thus selected so that both robots are not in full extension, as seen in Figure 14, which solved the resonance problem.

3.3.4 Hole-drilling

The last step of the fabrication process is the drilling of pilot holes. A standard beam has 12 holes: 6 longitudinal holes and 6 transversal holes. The gripping robot carries the beam towards a fixed router, visible in Figure 15. This choice introduces a potential risk of collision between the router and the gripper. The conclusions are similar to the rough cut stage: large deviations from perpendicularity between beams should be avoided.

3.4 Calibration

A specific calibration procedure is required for the multi-robotic cell, which permits both robots to share a common base frame. Several constraints have defined the calibration methodology, the main ones being:

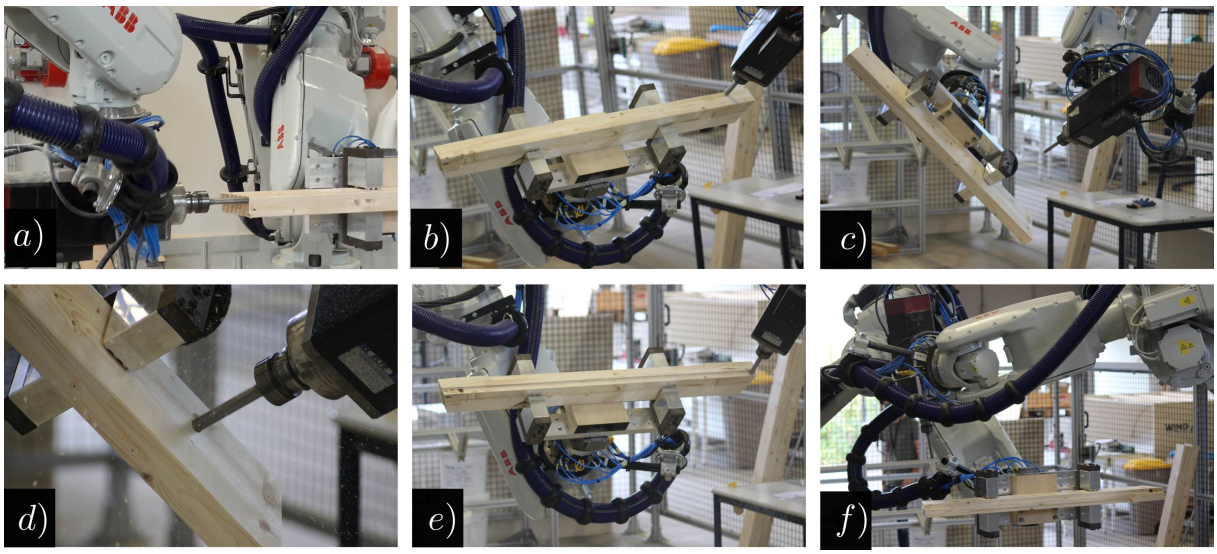

Fig. 13 Milling steps: a) tenon milling, b) top surface, c & d) mortises, e) grooves, f) bottom surface.

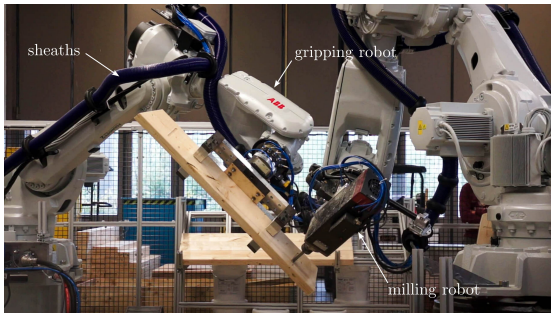

Fig. 14 Milling of a mortise: *gripping robot* with beam (left) and *milling robot* with spindle (right).

- cost-efficient tip-type calibration tool (no calibration via sensors)
- non-measurable distortion of the track over time
- non-measurable deformation and variation due to various vibrations during the processes
- large working area for main machining operations (operations 2 to 7).

The method consists in the seven steps.

- **Rough identification of the difference in positioning** between the two base frames.
- **Rough definition of the work area**. The greater the volume, the more difficult it is to achieve great precision because of the accumulation of various deformations.
- **Accessible region simulation and work volume maximization**. The goal of this step is to find the orientation of both robots for each vertex of the 3D polygon that describes the volume of work. The operator looks for a normal in a cone which corresponds to the set of attainable normals at any given point. The orientation around the normal is free. A margin of movement is let to adjust the position of the fixed robot afterwards. There is no restriction on the position of the chariot of the mobile robot. As a result, the observed volume includes track deformation.
- **Calibration of the two measuring tips** and their declaration as tools is then carried out. This step contributes a lot to the fineness of the calibration because it includes a parametric identification of tool's weight and center of gravity which let us have a robust dynamic model for each robot. The use of ABB's *Absolute Accuracy* option guarantees high precision in positioning, even in critical situations where the robot configuration is adverse.
- **Position measurement**: Once all positions have been found and the tool-path between each vertex is simulated, a routine is performed. It consists in moving the robot on track on each of the ten vertices. The fixed robot is then moved to the same position at a safe distance and manually adjusted until the two points touch. For each known point in the mobile robot base frame, the corresponding point in the fixed robot is recorded.

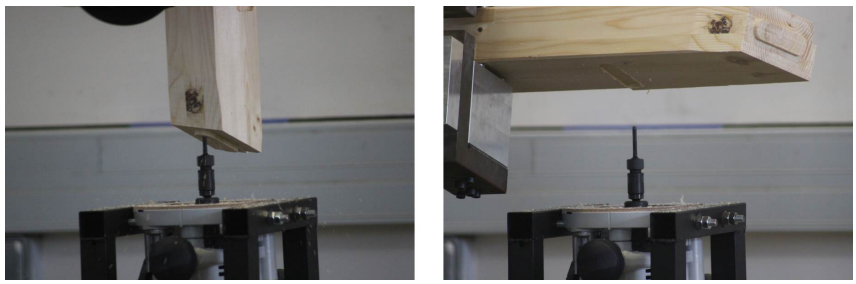

Fig. 15 Hole-drilling step: longitudinal and transversal pilot holes.

- **Optimal fitting of the base frames** with the least-squares method.
- **Declaration of the fixed robot base frame** in the track base frame.

This method guarantees an accuracy smaller than 1 mm between the measurements of the machined and theoretical parts. The calibration strategy can thus obtain satisfactory results for rather large building components at a reduced cost since it does not rely on external sensors. An alternative to this calibration would have been to use laser trackers [55], cameras [56], or a combination of laser beams with cameras [57]. The calibration procedure is time-consuming and relies on the operator's skill during peak-to-peak measurement, which limits its accuracy. However, the least-squares method decreases the error. Implementation of this routine allows a cell of this type to be calibrated in about two hours and requires no sensors. It is essentially based on the minimization of measurement errors by the least-squares method, and the accuracy of tool calibration and the associated dynamic model.

The precision requires re-calibrating the working area when a new job starts. The cell undergoes minimal temperature variations, but the slight length variations of the track and robots and the vibrations generated by machining operations are non-negligible compared to the aimed accuracy.

3.5 Integration and detail workflow

The CAD/CAM workflow operated at different representation complexities. Constructive or design problems, like panel planarity, or preliminary structural design were addressed with simple data structures during the *design geometry* stage and implementations (meshes or simple extensions of meshes), while others require a full simulation of the fabrication process.

The preliminary form-finding is based on mesh representation, in the fashion of most work in architectural geometry. It combines the marionette technique, which guarantees facet planarity for quadrangular meshes [58, 46] and a form-finding technique for nexorades introduced by the authors in a previous publication [59]. This data structure is also compatible with an automated construction of a finite element model, which was used to ensure compliance with Eurocode 5. Details about the preliminary design can be found in [43]. The software integration was performed through the coding of a C# library that was used to generate Grasshopper components. Figure 16 shows the main objects coded in the library. A class for *nexorades* has been created: it uses a particular data structure based on the fact that each beam only has at most 4 adjacent beams in a nexorade, as shown in the picture. This remark leads to an efficient way to encode connectivity between components of a nexorade. The other peculiarity of nexorades is the nodal *eccentricity*, which means that the axes of two adjacent beams are not concurrent: this requires the storage of two points to keep track of the relative positions of the members. The main methods implemented consisted in transforming a mesh into a *nexorade* and performing the form-finding with the translation technique.

However, manufacturing constraints require more in-depth modeling, and the use of a digital robotic twin is necessary to ensure the feasibility of the fabrication. The data structure listed in Figure 16 was thus later enriched with more information during the *Fabrication geometry* stage. For example, the panel thickness, or position of screw axes are not required in early design iterations but are needed to generate the toolpaths. Other pieces of information that are added include groove overlapping distance with beam, clearance,

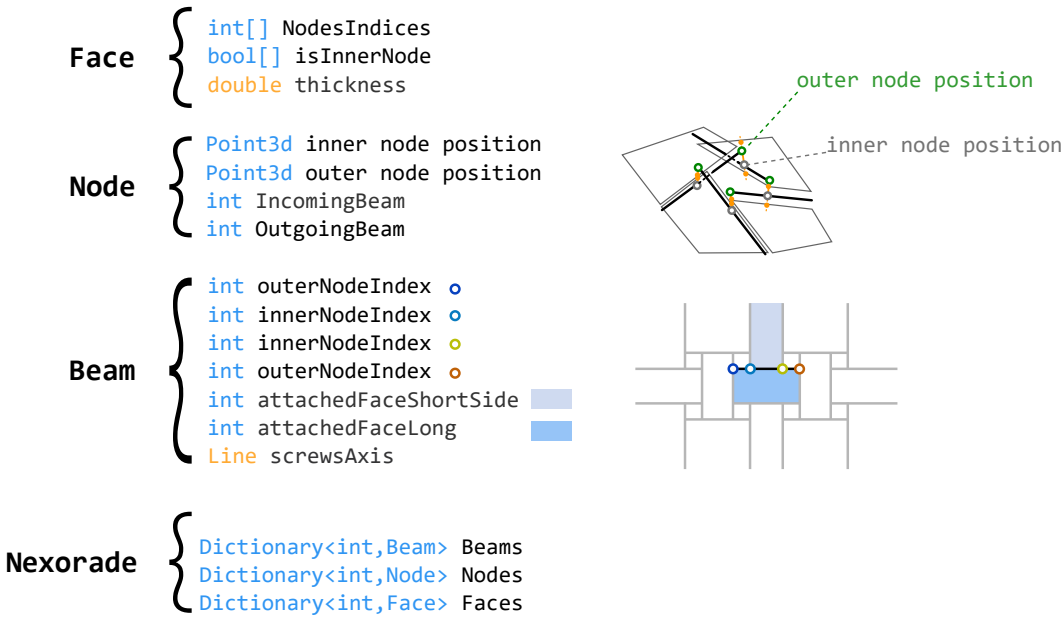

Fig. 16 Main objects used during the design (in bold) and their properties (under brackets). Blue types refer to data used during the *design geometry* stage, while orange types refer to data used during the *fabrication geometry* stage (non-exhaustive list).

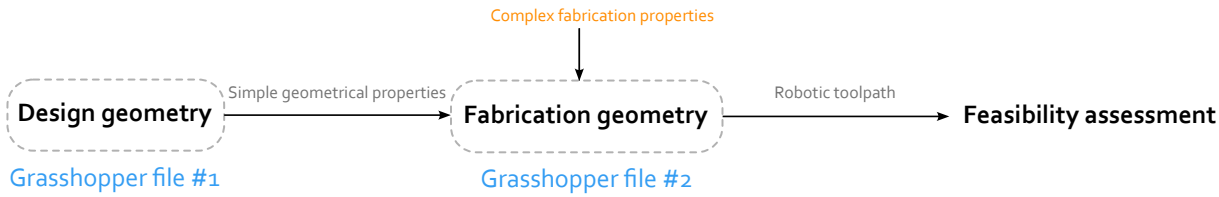

Fig. 17 Simple overview of the computational workflow.

beam local axes, position and depth of pilot holes, dimensions of tenons and mortise, dimensions of the milling cutter, position of Tool Center Point with respect to robot end axis, the position of the beam with respect to the tool center point, etc. It was thus possible to iteratively enrich the data structure thanks to the object-oriented programming approach. The computational workflow is illustrated in Figure 17: the preliminary design was done with a first Grasshopper™file, which allowed to interactively manipulate the target geometry and form-finding of the nexorade. When the design team was satisfied, they could use a second Grasshopper™file where fabrication data could be set as an input to compute the robotic tool-path and check the feasibility of the design.

The variability of pieces created additional difficulty: it was not possible to find a generic and optimal strategy for the milling stages (3-7). Clustering was performed based on the length and angle similarities between beams, and for most beams, an automated procedure could be generated. Specific cases, where the length of the beam was either smaller than 1300mm, or larger than 1700mm were treated manually in the 3D modeling environment, with visual feedback on potential collisions and accessibility. Figure 18 shows the visual feedback in the 3D modeling environment. Here, the user specifies a region where the mortise should be milled and the inverse kinematics is solved by HAL Robotics software [25]. When a trajectory was not feasible, the designer could simply change the holding position of the beam with a slider in *the second Grasshopper file*, or the milling area by specifying a point in the 3D modeling environment within the calibration volume. From our experience, a problematic case could be

solved in a few minutes. This was more reliable than coding a generic optimization scheme, given the low number of problematic beams.

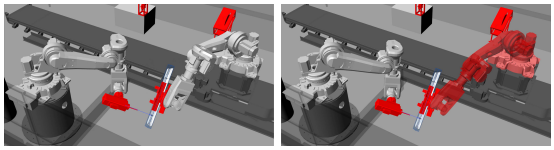

Fig. 18 Visual feedback of feasibility of robot configuration (left: a feasible position, right: a non-feasible position).

4 Results and productivity analysis

The case study allowed us to gather information on the use of materials, equipment and labor during manufacturing and assembly. This section presents a productivity analysis based on the case study, as well as a feedback on dimensional accuracy of the manufacturing strategy.

4.1 Geometrical control and tolerances

The selection of appropriate tolerances and clearances in a fabrication process is decisive for the choice of a manufacturing strategy. In the case study presented in this paper, the coupling between milling speed and robot position was crucial for the achieved precision. The intended tolerance for the case study is 1 mm. It is far from the manufacturing tolerances reached in industrial robotics, but the additional precision comes at the cost of additional investments in sensors. The high hyperstaticity of the pavilion required careful geometric control of each fabrication step:

- at member scale, about 8 measures (4 lengths and 4 angles) were checked with millimetric accuracy (or equivalently, 10 milliradians);
- at panel scale, before screwing, the geometry of the four edge members lining the panel was adjusted so that the panel (whose diagonal length accuracy was systematically checked and within ± 1 mm) fitted within the 2 mm tolerance of the grooves;
- at structure scale, the anchor plates were fixed beforehand by the traditional triangulation method. The plates were equipped with slotted holes insuring ± 3 mm in each direction to make up for accuracy.

A measuring campaign was carried out with a laser scanner and photogrammetric 3D reconstruction. The two techniques were used for pedagogical purposes and comparison of their relative accuracy. The first 3D point cloud from the laser scanner was established from four positions to get a complete picture of the inside and outside of the pavilion. The resulting accuracy is about ± 1 mm. The second point cloud was created using the free photogrammetry software *Micmac* [60] and from a set of 134 photos (5400 x 3600). The resulting accuracy is also about ± 1 mm in every direction. A set of 25 stationary targets had been placed around the pavilion to be localized by traditional tachometer techniques and to allow for geo-referencing of both point clouds. Globally, the two point clouds are identical, with an average gap close to 1 mm.

The point cloud, shown in Figure 19, was then compared to the initial 3D model in Rhino. The legend indicates large deviations, but it can be seen that those deviations occur at the edges of beams, where the measure is less precise. The average gap is about -6 mm (the 3D model being above the cloud). From the analysis of the signed distance between the mesh and cloud, one can see that:

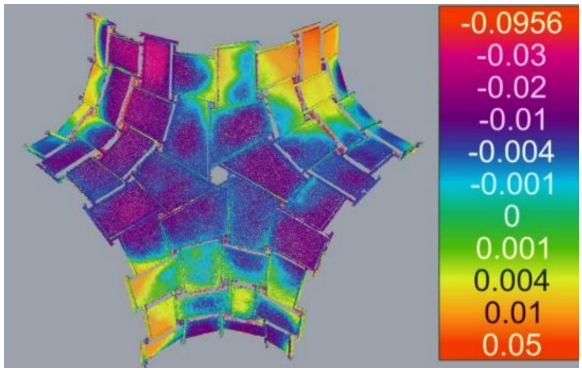

Fig. 19 Signed distance between the point cloud obtained from photogrammetry and the planned geometry. The colour scale is non-linear to better highlight deviations between -1cm and +1cm.

- the unprotected plywood panels have creep and present a residual deflection in the middle of

approximately 4 mm relative to the initial panel plane;
- part of this gap can be explained by the deformation induced by gravity (2 mm at crown according to the mechanical model with Karamba3d);

The quality of the execution at the structural scale is thus globally very satisfactory, and the deviation from the planned geometry and the measured geometry is estimated to be 2mm after accounting for panel deflection. No difficulty was encountered during assembly, which illustrates the geometrical faithfulness of the manufacturing process.

4.2 Cost hypothesis

The work hours are split between different workstations:

- Automated equipment supervision
- Fabrication preparation
- On-site assembly

The workstations *Automated equipment supervision* and *On-site assembly* rely on the available equipment. We used indeed academic facilities with a scale and constraints different from industrial installations.Two people supervised the robotic cell, which explains the high supervision cost in our case study. Additionally, calibration was time-consuming, and could easily be improved with state-of-the-art methods, for example, by using cameras [56].

4.3 Construction phase

The costs for material, equipment, and labor for the fabrication and assembly of the prototype are reported in Table 1 and Table 3. Three scenarios of production are identified.

- A conservative scenario considers a milling time of 40 minutes per beam and a typical work day of 8 hours for the depreciation of the equipment;
- An intermediate scenario considers a milling time of 20 minutes per beam and a typical work day of 12 hours for the depreciation of the equipment;
- An optimistic scenario considers an optimized milling time of 10 minutes per beam and a typical work day of 12 hours for the depreciation of the equipment;

The three scenarios are chosen to reflect three phases of the experience curve of the manufacturing process. The first milling tests were done at a reduced speed corresponding to the pessimistic scenario to control the absence of collisions. Speed was gradually increased over time, essentially for the robots' movements between the workstations. The last beams were machined in ten minutes. In this case study, batch size is thus an important aspect of productivity analysis: the reconfiguration of the cell causes the ramp-up to be slower than in conventional robotic cells.

The cost is estimated for three aspects: the equipment, which considers the investment made to acquire the robots, specific tools, computers, and software licenses; man-hours during the fabrication and assembly; and the material. Both equipment and labor depend on the chosen scenario, while the amount of material is independent of the production time.

4.4 Material

Table 1 recalls the breakdown for material cost. The total price is 58€/m^2 besides foundation support and foundation, most of which is for the plywood panels, which is within the range of other academic prototypes of free-form structures. For example, a gridshell covered by a concrete shell costs 56 €/m^2 for a span of 2 meters [61].

Description	Quantity	Cost
Timber GL24h,	0.99 m^3	788€
Panels	0.93 m^3	1482€
Screws for beam attachment	612	612€
Screws for panel attachment	2400	50€
Foundation support	32	480€
Total		3412€

Table 1 Material cost for the pavilion, based on the purchase cost.

Table 2 displays the price and depreciation period of the equipment. The amortization period is based on the average lifespan of industrial equipment, assuming 230 working days of the facility per year.

Description	Cost	Depreciation period
Equipped robotic cell	180 000€	8 years
CNC router	25 000€	8 years
Computers	2 000€	3 years
Software	2 000€	1 year
Roughing cutters	600€	24 hours

Table 2 Price of the equipment used in the proposed ROD workflow.

4.5 Fabrication phase

The labor costs unrelated to the supervision of the manufacturing process (robot and CNC) are detailed in Table 3. The man hours are expressed for three workstations. An equivalent price is estimated based on the average cost of work in France at the time of completion of the project, which is 34€/h, according to INSEE [1]. The values are indicative since the various tasks require different levels of skills.

In the pessimistic production scenario, shown in Table 6, the robotic cell is used for 86 hours and requires 172 hours of supervision, which would represent 47% of the total labor (365 hours). The depreciation cost represents half of the raw material cost, and cannot be neglected in the cost estimation.

In the intermediate scenario, shown in Table 7, the robotic cell is used for 44 hours and requires 88 hours of supervision, which represents 31% of the total labor of the project (281 hours).

In the optimistic scenario of beam production, the robotic cell is used for 23 hours and requires 46 hours of supervision, which represents 19% of the total labor of the project (239 hours). The material depreciation is then negligible compared to raw material cost and labor.

The panel milling took a total of 60 hours, with approximately 15 minutes required for preparing the panels (see table 3) and 45 minutes for milling. This is objectively a long milling time, compared to industrial processes [62], due to the antiquated state of the CNC available. The panel cutting preparation and milling supervision represent between 20% and 30% of labor depending on the scenario. It is an obvious point for improvement in the fabrication process since the panels require extremely simple cuts.

[1] https://www.insee.fr/en/statistiques/serie/001565188 and https://www.insee.fr/en/statistiques/1304009

The efficiency of the milling process directly impacts the need for human supervision of the process, as shown in Table 8. For safety reasons, two people must indeed be at any time of the milling process in the vicinity of the milling equipment. The evaluation of the cost of design development is more difficult to assess since parts of the design process required research work (e.g. the form-finding method for nexorades [59]).

4.6 Productivity of fabrication method

Several trends can be observed in productivity. First, adapting a robotic cell to a new process involves a ramp-up in productivity, which makes the final cost dependent on the batch size. Strong differences in manpower and depreciation costs were observed depending on the productivity scenario. This tempers the economical interest of extreme customization in complex systems involving several robotic processes. Second, a more adequate CNC router could have improved the panel milling operation. Third, it appears that the connection between beams and panels becomes one of the most time-consuming actions in the intermediate and optimistic scenario (although this stage was conducted concurrently with robotic fabrication and did not result in production delay). This may advocate for the integration of this action in the robotic process, and thus for more versatility, the tools used for the BUGA Pavilion are a good blueprint for an assembly station, and some comments are made in Section 5.4. Finally, the on-site assembly time, omitting the on-site positioning and foundation preparation, remained low. Table 3 shows that roughly one person-hour per m^2 is necessary for assembly, and the added value was indeed shifted from the construction site to the factory, as initially intended.

5 Discussion

5.1 Complex trajectories simulation

The modeling of the trajectories of the robots is a complex task, as several parameters may affect output quality. The simulation should therefore go beyond the simple solving of an inverse kinematic problem. For example, the resonance of the robot under milling loads would require finite element

Workstation Beam prefabrication					
Description	Time	People	Quantity	Total time [h]	Cost [€]
Setting the beam in the feeder	2'00"	1	102	3.4	115.6€
Picking the beam from the feeder	1'00"	1	102	1.7	57.8€
Quality control	3'00"	1	102	5.1	173.4€
Labeling of the beam (writing+deposition)	2'00"	1	102	3.4	115.6€
Sending the beam to site	1'00"	1	102	1.7	57.8€
Total				15.3	520.2€
Workstation Panels prefabrication					
Description	Time	People	Quantity	Total time [h]	Cost [€]
Anchoring the panel into the CNC	5'00"	1	60	4	136€
Quality control of the file	1'00"	1	60	1	34€
Label deposition	1'00"	1	60	1	34€
Remove the panel from the CNC	5'00"	1	60	4	136€
Fabrication of a guide for pre-drill	2'00"	1	8	2	68€
Drilling of pilot holes for panels/beams attachment	4'00"	3	60	12	408€
Total				24	816€
Workstation Site assembly					
Description	Time	People	Quantity	Total time [h]	Cost [€]
On-site positioning	5:00'00"	4	1	20	680€
Foundation pre-drills	5'00"	2	32	5.3	181.3€
Lowering of the centring	4:00'00"	6	1	24	816€
Setting a panel and mechanical attachment	5'00"	1	60	5	170€
Picking a beam from stock and placing	2'00"	1	102	3.4	115.6€
Mechanical attachment between beams	1'00"	2	102	3.4	115.6€
Picking a panel from stock	2'00"	1	60	2	68€
Placing a panel	1'00"	1	60	1	34€
Drilling of pilot holes for panels/beams attachment	4'00"	3	60	12	408€
Total				76.1	2588.5€
Subtotal prefabrication and assembly				115.4	3924€
Supervision (15%)				17.3	588.5€
Total prefabrication and assembly				**133**	**4513.4€**

Table 3 Labor cost, excluding supervision of the machining process.

Workstation panel pre-fabrication		
Description	Time	Equivalent cost (depreciation)
Panel milling	60h	95€
Tools	60h	200€
Total panel pre-fabrication		295€

Table 4 Depreciation cost for the CNC for all the scenarios.

Workstation beam pre-fabrication		
Description	Time	Equivalent cost (depreciation)
Total fabrication time	68 h	831€
Calibration time	18 h	220€
Tools		200€
Total beam pre-fabrication		1251€

Table 5 Depreciation cost and tools for the pessimistic scenario of production.

analysis. In practice, the sheaths on the robotic arm, shown in Figure 14, were subject to instabilities during the various re-orientations of the robot. They also restricted the rotation along the fourth axis of the robot. This led to the introduction of kinematic constraints to avoid those

Workstation beam pre-fabrication		
Description	Time	Equivalent cost (depreciation)
Total fabrication time	34h	277€
Calibration time	10h	81€
Tools		200€
Total beam pre-fabrication		558€

Table 6 Depreciation cost and tools for the intermediate scenario of production.

Workstation beam pre-fabrication		
Description	Time	Equivalent cost (depreciation)
Total fabrication time	17h	139€
Calibration time	6h	49€
Tools	8h	200€
Total beam pre-fabrication		388€

Table 7 Depreciation cost and tools for the optimistic scenario of production.

problems. However, the simulation of the deformation of sheaths could be done to predict, and later avoid those instabilities.

5.2 Integration in the conventional design scheme

Most of the time spent on the case study concerned the preliminary and detailed design, either to determine the manufacturing strategy described in Section 3 or to generate the toolpaths. The adjustment of the geometry to comply with manufacturing and structural constraints also requires high-end engineering time with the development of tailor-made form-finding tools [43]. The pavilion described in this article is an academic project with open research questions at its premises, this remark should thus be tempered for more common building applications. Two limitations arise with the current state-of-the-art in the building industry.

First, the simulation of the manufacturing process cannot usually be done during preliminary design phases when the contractors and thus the production means are not precisely known. The main consequence is the multiplication of iterations between contractors and designers to guarantee both ease of manufacturing and compliance with the design requirements. This limitation can be addressed by the introduction of simplified metrics during the very early stages of design, which are yet to be properly defined in a discrete geometry framework, similar to constraints such as facet planarity. Some advances in other fields, like computational mechanics could be leveraged to that effect. Figure 20 shows both the complex feasible domain in cutting angles α, β (white filling, with black contour) and a possible simplification with a rectangular domain. The feasible domain is initially a polyline with 30 vertices, which may be too much information to process in practice. Although the rectangular domain does not contain all feasible designs, it has the advantage of being described by only 4 inequalities: $\alpha_{min} < \alpha < \alpha_{max}$ and $\beta_{min} < \beta < \beta_{max}$. It is also convex and much easier to implement for various actors who are not necessarily experts in non-convex programming. In the case study presented in this paper, the rectangular domain was found heuristically, but systematic approaches, like the one based on area maximization of the rectangle, can be implemented [63]. To go further, Bleyer and de Buhan approximated complex convex surfaces by summing ellipsoids. The main advantage of their approach is that it is compatible with second-order cone programming problems, an important subset on convex programming [64]. More importantly, this limitation could be addressed by a closer collaboration between the design team (architects, structural engineers) and prefab companies (specialists in manufacturing) during the early stages of design [11].

Second, the deployment of a fully digitized workflow for design, production and assembly, within existing modeling tools is rarely observed, due to the specialization of software employed by the different actors of a construction project. There is therefore a need for a new digital framework integrating 3D-modeling, geometrical rationalization, structural analysis, and fabrication simulation. The digital workflow proposed by the authors, based on a specific C# library, on Rhinoceros and HAL Robotics is an example of such workflow.

	Number of hours	Number of people	Total time	Equivalent cost
Panel milling	45h	1	45h	1530€
Pessimistic scenario	86h	2	172h	5848€
Intermediate scenario	44h	2	88h	2992€
Optimistic scenario	23h	2	46h	1564€

Table 8 Labor costs induced by the supervision of the milling process.

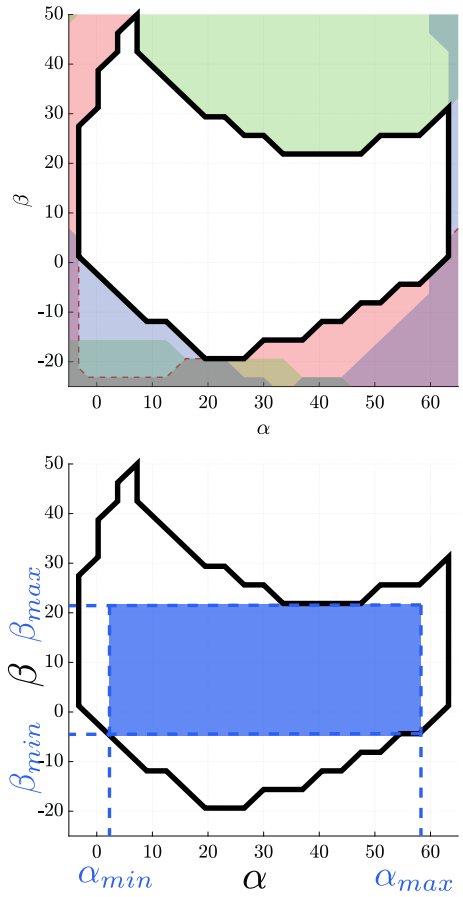

Fig. 20 Feasible geometrical domain for milling (top) and a rectangle in the domain (bottom).

5.3 Scalability

The workflow presented in this paper allowed for the design and construction of a 50m^2 pavilion, with beam lengths varying between 1.2m and 1.8m. The robotic setup chosen does not allow for shorter lengths, and longer beams may yield vibrations during milling due to eccentricity. The upper bound for beam lengths is evaluated at 2 meters. The modularity of the gripper, shown in Figure 4, would allow for an adaptation to other cross sections, with a width up to 24cm.

In the case study presented in this article, the payload of the robots (150kg) exceeds by far the weight of the manipulated components (5kg), even when considering the weight of the gripper (40kg) and the range of lengths chosen is characteristic of cladding components. These observations show that there is some room for upscaling the process to larger buildings, the main question being the evolution of the weight of the components with the span. A parametric study on this matter has been performed in [43] and shows that the surface weight of shell-nexorade hybrid follows a linear trend with the span of the structure whereas classical nexorade follows a non-linear trend. With a span of 20 meters, the surface weight remains less than 30kg/m^2, and thus the weight of the components would remain less than 10kg. Therefore, the manufacturing strategy proposed in this paper could be applied to a large-scale structure with little adaptation of the robotic cell.

Table 9 displays a comparison of key figures between our approach and two larger-scale pavilions fabricated with robotic platforms. The first one is the *Sequential Roof* built at ETH Zurich, and the second is the *BUGA Pavilion*, which was fabricated with a flexible mobile platform [26]. The pavilion presented in this article results in highly efficient use of material, with the lowest surface weight, even when scale effects are factored in. The three production scenarios have been taken into account: only the intermediate and pessimistic scenarios are competitive with the two previous studies. This confirms that ramp-up should be considered in productivity analysis, as small-scale production is less likely to reach peak productivity. The higher productivity of our approach in the optimistic scenario should also be tempered, as we only focus on single components, whereas the two former projects involve an assembly of sub-components. However, the productivity

analysis has shown that on-site assembly was not the most time-consuming stage of the fabrication.

5.4 Assembly

The case study presented in the previous section was manually assembled. The assembly process could also be automated both in the context of large-scale prefabrication and on construction sites, with several adjustments to the design of the components. In both cases, the need for accuracy requires specific measurement and instrumentation, which were not needed during machining.

Fig. 21 Timber pavilion with simple beams and complex connectors.

(a) Node assembly on a fixed support

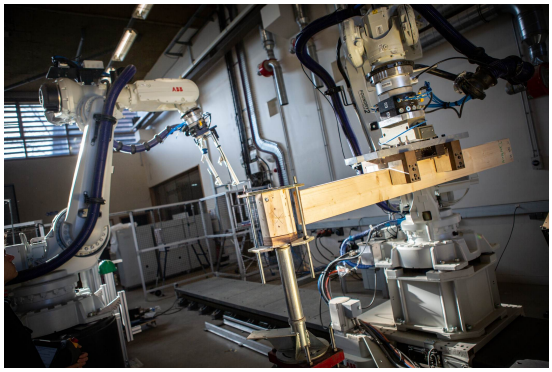

(b) Beam assembly

Fig. 22 Discrete assembly with a gripper (photo: Ecole des Ponts ParisTech/Stefano Borghi)

The cell configuration, where the robot is used as a mobile reference frame for each beam, has been used in other case studies. Figure 21 shows a timber pavilion with nodal connectors and timber beams, which were cut with the saw and gripper presented in this article (steps 1,2 and 8).

The cell can also be used during the assembly, which would immediately follow the machining step (and replace workstation 9). This limits the need for a positioning system, as each beam can be successively assembled with the required precision. An assembly on fixed support in the robotic cell is shown in Figure 22. A recent example of mobile construction platform illustrates the potential for on-site milling and assembly [36]. The platform uses more sensors than the one presented in this article, with the benefit of higher flexibility and accuracy.

The in-situ assembly of components assumes that all the components are pre-fabricated and later assembled into larger units on the construction site. The main question for the integration in a ROD workflow, apart from classical problems related to in-situ construction robots, is the definition of a reference frame for each component. Several options seem available for the construction

- Use a specific feeder that allows for a straightforward pick-and-place operation. In non-standard projects, the fabrication of such a feeder might be too costly.
- Use a combination of markers and/or calibrated sensors that can relocate each beam. The main drawback is the sensitivity to calibration in an uncontrolled environment, as well as the potential cost of sensors used for accurate 3D localization.
- Use low-tech sensors combined with algorithms for precise object localization [65].

The latter option seems promising since a relative localization between a brick and a manipulator with a precision of 2mm can be achieved without manual calibration thanks to deep learning in

	Sequential Roof	BUGA Wood Pavilion	This work
Structure	Truss-Beam	Segmented Shell	Shell-nexorade hybrid
Span	15 m	30 m	7.5m
Robotic System	Fixed Gantry (3-axis)	Flexible Platform (15 axis)	Flexible Platform (13-axis)
Production Time	63 min/m^2	41 min/m^2	103-53-28 min/m^2
Material Usage	71 kg/m^2	38 kg/m^2	7 kg/m^2

Table 9 Comparison of key timber prefabrication benchmarks of Sequential Roof [23] , BUGA Wood Pavilion [36], and this case study. The three production times correspond to the pessimistic, intermediate and optimistic scenarios.

[65]. The main difficulties with this approach are the software integration, the generalization to the localization of non-standard building components and the reliability assessment in an industrial context. Finally, it should be noted that the milling stage is also likely to be modified if the assembly is performed by robots, either to incorporate mechanical coding or to simplify the design of the end-effector, which would likely differ from the gripper used for the milling stages [66].

6 Conclusion

This paper has investigated the application of ROD to free-form timber structures and identified some practical limitations to be considered by designers. The flexibility of manufacturing equipment and of the software environment were identified as key parameters in the development of a true *fabrication-aware design approach*. A design for a 13-axis robotic cell was proposed and applied to the construction of a 50 m^2 pavilion with a doubly-curved shape. The cell uses a robot with a pneumatic gripper that acts as a reference frame for the component that navigates the cell. The building components were fabricated with millimetric accuracy and were assembled onsite with faithfulness to the planned geometry, as demonstrated by a 3D scan of the pavilion.

Object-oriented programming was used throughout the design process. The amount of information and the complexity of calculation increased throughout the project. In order to keep an interactive design tool, simplified constructability metrics have been created for the specific needs of the project. The flexibility of industrial manipulators and the control software allowed for several iterations of the layout of the robotic cell, which made manufacturing possible.

A productivity analysis was conducted and showed that labor was shifted from the construction site to the factory. It also showed that the manual calibration of the different tools is one of the most time-consuming steps of the fabrication process. Solutions that could automate calibration, with external sensors could thus be used to increase productivity.

Future work includes the integration of manufacturing constraints in earlier stages of design. However, this latter challenge seems to be an organizational issue in the construction industry rather than a technical one. Dialogue between production and design teams remains essential for the success of complex projects involving digital fabrication.

References

[1] Thomas Bock and Silke Langenberg. Changing building sites: Industrialisation and automation of the building process. *Archit. Des.*, 84(3), 2014.

[2] Andrew BORGART. New challenges for the structural morphology group. *Journal of the International Association for Shell and Spatial Structures*, 51(3):183–189, 2010.

[3] Jean-François Caron, Olivier Baverel, Cyril Douthe, Romain Mesnil, and Tristan Gobin. Proposals to make complex structures affordable. pages S5–63–S5–70, 2018.

[4] Jan Knippers and Thorsten Helbig. Recent developments in the design of glazed grid shells. *International Journal of Space Structures*, 24(2):111–126, 2009.

[5] Nannan Guo and Ming C Leu. Additive manufacturing: technology, applications and research needs. *Frontiers of Mechanical Engineering*, 8(3):215–243, 2013.

[6] Helmut Pottmann, Michael Eigensatz, Amir

Vaxman, and Johannes Wallner. Architectural geometry. *Computers & Graphics*, 47:145–164, 2015.

[7] Yang Liu, Helmut Pottmann, Johannes Wallner, Yong-Liang Yang, and Wenping Wang. Geometric modeling with conical meshes and developable surfaces. In *ACM SIGGRAPH 2006 Papers*, pages 681–689. 2006.

[8] Helmut Pottmann, Yang Liu, Johannes Wallner, Alexander Bobenko, and Wenping Wang. Geometry of multi-layer freeform structures for architecture. In *ACM SIGGRAPH 2007 Papers*, SIGGRAPH '07, page 65–es, New York, NY, USA, 2007. Association for Computing Machinery.

[9] Hans Schober. *Transparent shells: Form, topology, structure*. John Wiley & Sons, 2015.

[10] Guy Austern, Isaac Guedi Capeluto, and Yasha Jacob Grobman. Rationalization methods in computer aided fabrication: A critical review. *Automation in Construction*, 90:281–293, 2018.

[11] Thomas-Alexander Bock. Robot-oriented design. In Rokuro Ishikawa, editor, *Proceedings of the 5th International Symposium on Automation and Robotics in Construction (ISARC)*, pages 135–144, Tokyo, Japan, June 1988. International Association for Automation and Robotics in Construction (IAARC).

[12] Thomas Bock and Thomas Linner. *Complex Products in Other Industries and Relevance of Fixed-Site/On-Site Manufacturing Technology*, page 125–155. Cambridge University Press, 2015.

[13] Thomas Bock and Thomas Linner. *Robot-oriented design: Design and management tools for the deployment of automation and robotics in construction*. Cambridge University Press, 2015.

[14] Thomas Bock and Thomas Linner. *Robotic Industrialization: Automation and Robotic Technologies for Customized Component, Module, and Building Prefabrication*. Cambridge University Press, 2015.

[15] Fabian Scheurer, Hanno Stehling, Franz Tschümperlin, and Martin Antemann. Design for assembly–digital prefabrication of complex timber structures. In *Proceedings of IASS Annual Symposia*, volume 2013, pages 1–7. International Association for Shell and Spatial Structures (IASS), 2013.

[16] Ingrid Bertin, Romain Mesnil, Jean-Marc Jaeger, Adélaïde Feraille, and Robert Le Roy. A bim-based framework and databank for reusing load-bearing structural elements. *Sustainability*, 12(8):3147, 2020.

[17] Yannick Masson and Laurent Monasse. Existence of global chebyshev nets on surfaces of absolute gaussian curvature less than 2π. *Journal of Geometry*, 108(1):25–32, 2017.

[18] Cyril Douthe, Romain Mesnil, Hugo Orts, and Olivier Baverel. Isoradial meshes: Covering elastic gridshells with planar facets. *Automation in Construction*, 83:222–236, 2017.

[19] Achim Menges, Tobias Schwinn, and Oliver David Krieg. *Advancing wood architecture - a computational approach*. 2016.

[20] Zachary Mollica and Martin Self. Tree fork truss. *Advances in Architectural Geometry*, 2016:138–153, 2016.

[21] Thibault Schwartz, Joshua Bard, Madeline Ganon, Zack Jacobson-Weaver, Michael Jeffers, and Richard Tursky. In *Robotic Fabrication in Architecture, Art and Design 2014*.

[22] Volker Helm, Michael Knauss, Thomas Kohlhammer, Fabio Gramazio, and Matthias Kohler. Additive robotic fabrication of complex timber structures. In *Advancing Wood Architecture: A Computational Approach*, pages 29–43. Routledge, 2016.

[23] Jan Willmann, Michael Knauss, Tobias Bonwetsch, Anna Aleksandra Apolinarska, Fabio Gramazio, and Matthias Kohler. Robotic timber construction — expanding additive fabrication to new dimensions. *Automation in Construction*, 61:16 – 23, 2016.

[24] Thibault Schwartz. HAL: Extension of a visual programming language to support teaching and research on robotics applied to construction. *Rob|Arch 2012*, pages 92–101, 2013.

[25] Tristan Gobin, Sebastian Andraos, Thibault Schwartz, and Rémi Vriet. A framework for modelling, simulating and parametrically programming heterogeneous industrial machines. *Construction Robotics*, pages 1–8, 2022.

[26] Hans Jakob Wagner, Martin Alvarez, Abel Groenewolt, and Achim Menges. Towards

digital automation flexibility in large-scale timber construction: integrative robotic prefabrication and co-design of the buga wood pavilion. *Construction Robotics*, 4(3-4):187–204, 2020.

[27] Pierre Gilibert, Romain Mesnil, and Olivier Baverel. Rule-based generative design of translational and rotational interlocking assemblies. *Automation in Construction*, 135:104142, 2022.

[28] Anja Kunic, Roberto Naboni, Aljaz Kramberger, and Christian Schlette. Design and assembly automation of the robotic reversible timber beam. *Automation in Construction*, 123:103531, 2021.

[29] Thomas Kohlhammer, Aleksandra Anna Apolinarska, Fabio Gramazio, and Matthias Kohler. Design and structural analysis of complex timber structures with glued t-joint connections for robotic assembly. *International Journal of Space Structures*, 32(3-4):199–215, 2017.

[30] Christopher Robeller and Yves Weinand. Interlocking folded plate–integral mechanical attachment for structural wood panels. *International Journal of Space Structures*, 30(2):111–122, 2015.

[31] Christopher Robeller, Mina Konaković, Mira Dedijer, Mark Pauly, and Yves Weinand. Double-layered timber plate shell. *International Journal of Space Structures*, 32(3-4):160–175, 2017.

[32] Olivier Baverel, Hoshyar Nooshin, Y. Kuroiwa, and G.A.R. Parke. Nexorades. *International Journal of Space Structures*, 15(2):155–159, 2000.

[33] Olivier LS Baverel. *Nexorades: a family of interwoven space structures*. PhD thesis, University of Surrey, 2000.

[34] Fabian Scheurer. Getting complexity organised: using self-organisation in architectural construction. *Automation in construction*, 16(1):78–85, 2007.

[35] Samuel Leder, Ramon Weber, Dylan Wood, Oliver Bucklin, and Achim Menges. Distributed robotic timber construction: Designing of in-situ timber construction system with robot-material collaboration. *ACADIA 2019*, 2019.

[36] Hans Jakob Wagner, Martin Alvarez, Ondrej Kyjanek, Zied Bhiri, Matthias Buck, and Achim Menges. Flexible and transportable robotic timber construction platform – tim. *Automation in Construction*, 120:103400, 2020.

[37] Antoine Picon. *L'ornement architectural Entre subjectivité et politique*. Presses polytechniques et universitaires romandes, 2017.

[38] Thomas Bock and Thomas Linner. *Building Module Manufacturing*, page 66–71. Cambridge University Press, 2015.

[39] Mohammed M Mabkhot, Abdulrahman M Al-Ahmari, Bashir Salah, and Hisham Alkhalefah. Requirements of the smart factory system: A survey and perspective. *Machines*, 6(2):23, 2018.

[40] Elvis Hozdić. Smart factory for industry 4.0: A review. *International Journal of Modern Manufacturing Technologies*, 7(1):28–35, 2015.

[41] Johannes Braumann and Sigrid Brell-Cokcan. Parametric robot control: integrated cad/cam for architectural design. 2011.

[42] Ben Shneiderman. The future of interactive systems and the emergence of direct manipulation. *Behaviour & Information Technology*, 1(3):237–256, 1982.

[43] Romain Mesnil, Cyril Douthe, Tristan Gobin, and Olivier Baverel. Form finding and design of a timber shell-nexorade hybrid. In *Advances in Architectural Geometry 2018 (AAG 2018)*, Göteborg, Sweden, September 2018.

[44] Shabtai Isaac, Thomas Bock, and Yaniv Stoliar. A methodology for the optimal modularization of building design. *Automation in construction*, 65:116–124, 2016.

[45] Hanno Stehling, Fabian Scheurer, and Jean Roulier. Bridging the gap from cad to cam: concepts, caveats and a new grasshopper plug-in. *Fabricate 2014. Negotiating design and making*, pages 52–59, 2014.

[46] Romain Mesnil, Olivier Baverel, and Cyril Douthe. Marionette meshes: modelling free-form architecture with planar facets. *International Journal of Space Structures*, 32, 2017.

[47] Gunter Ullrich. Automated guided vehicle systems. *Information Systems Frontiers*, 17, 2015.

[48] Andreas Thoma, Arash Adel, Matthias Helmreich, Thomas Wehrle, Fabio Gramazio, and Matthias Kohler. Robotic fabrication of

bespoke timber frame modules. In *Robotic Fabrication in Architecture, Art and Design*, pages 447–458. Springer, 2018.

[49] Santiago Martínez, Alberto Jardón, Juan Gonzalez Victores, and Carlos Balaguer. Flexible field factory for construction industry. *Assembly Automation*, 2013.

[50] Thomas Bock and Thomas Linner. *Robotic industrialization: Automation and robotic technologies for customized component, module, and building prefabrication*. 2015.

[51] C. Douthe, M. Bagnéris, L. du Peloux, and R. Mesnil. Building freeform: A workshop experiment from design to fabrication. page 252 – 261, 2018.

[52] Romain Mesnil, Cyril Douthe, Olivier Baverel, Bruno Léger, and Jean-François Caron. Isogonal moulding surfaces: A family of shapes for high node congruence in free-form structures. *Automation in Construction*, 59:38–47, 2015.

[53] Romain Mesnil, Cyril Douthe, Olivier Baverel, and Bruno Léger. Morphogenesis of surfaces with planar lines of curvature and application to architectural design. *Automation in Construction*, 95:129–141, 2018.

[54] Romain Mesnil. A re-parameterization approach for the construction of domes with planar facets. *Journal of the International Association for Shell and Spatial Structures*, 59(4):286–295, 2018.

[55] Albert Nubiola and Ilian A Bonev. Absolute calibration of an abb irb 1600 robot using a laser tracker. *Robotics and Computer-Integrated Manufacturing*, 29(1):236–245, 2013.

[56] Hanqi Zhuang and Zvi S Roth. *Camera-aided robot calibration*. CRC press, 2018.

[57] Sun Lei, Liu Jingtai, Sun Weiwei, Wu Shuihua, and Huang Xingbo. Geometry-based robot calibration method. In *IEEE International Conference on Robotics and Automation, 2004. Proceedings. ICRA'04. 2004*, volume 2, pages 1907–1912. IEEE, 2004.

[58] Romain Mesnil, Cyril Douthe, and Olivier Baverel. Marionette meshes: from descriptive geometry to fabrication-aware design. *Advances in Architectural Geometry*, 2016.

[59] Romain Mesnil, Cyril Douthe, Olivier Baverel, and Tristan Gobin. Form finding of nexorades using the translations method. *Automation in Construction*, 95:142–154, 2018.

[60] Ewelina Rupnik, Mehdi Daakir, and Marc Pierrot Deseilligny. Micmac–a free, open-source solution for photogrammetry. *Open Geospatial Data, Software and Standards*, 2(1):1–9, 2017.

[61] Pierre Cuvilliers, Cyril Douthe, Lionel Du Peloux, and Robert Le Roy. Hybrid structural skin: prototype of a gfrp elastic gridshell braced by a fiber-reinforced concrete envelope. *Journal of the International Association for Shell and Spatial Structures*, 58(1):65–78, 2017.

[62] Emanuel Martinez Villanueva, Harshavardhan Mamledesai, Pablo Martinez, Peyman Poostchi, and Rafiq Ahmad. Design and simulation of an automated robotic machining cell for cross-laminated timber panels. *Procedia CIRP*, 100:175–180, 2021.

[63] Apurba Sarkar, Arindam Biswas, Mousumi Dutt, and Arnab Bhattacharya. Finding a largest rectangle inside a digital object and rectangularization. *Journal of Computer and System Sciences*, 95:204–217, 2018.

[64] Jeremy Bleyer and Patrick de Buhan. Yield surface approximation for lower and upper bound yield design of 3d composite frame structures. *Computers & Structures*, 129:86–98, 2013.

[65] Vianney Loing, Renaud Marlet, and Mathieu Aubry. Virtual training for a real application: Accurate object-robot relative localization without calibration. *International Journal of Computer Vision*, 126(9):1045–1060, 2018.

[66] Jürgen Andres, Thomas Bock, Friedrich Gebhart, and Werner Steck. First results of the development of the masonry robot system rocco: a fault tolerant assembly tool. In *Automation and Robotics in Construction XI*, pages 87–93. Elsevier, 1994.